Chemistry—Methods

Research Article
doi.org/10.1002/cmtd.202400057

Chemistry Europe
European Chemical Societies Publishing

www.chemistrymethods.org

Determination of Boron Content in Surface Paintings From Historical Stained-Glass Windows

Laura Maestro-Guijarro,[a, b] Mercedes Sedano,[c] Nadine Schibille,[d] Trinitat Pradell,[e] Marta Castillejo,[a] Mohamed Oujja,*[a] and Teresa Palomar*[c, f]

Stained-glass windows are often painted with grisailles and enamels. These glassy materials have a low melting temperature and are fixed to the base glass by firing processes. Lead and/or boron are commonly added to the painting material to lower their melting temperature so that they can melt without deforming the glass support. In the present study, model glass samples (with well-known boron content), replica and historical materials were analysed for their composition using Laser Ablation Inductively Coupled Plasma Mass Spectrometry (LA-ICP-MS) and Laser Induced Breakdown Spectroscopy (LIBS). The imprint left on the analysed samples after laser irradiation was observed using optical profilometry. The feasibility of using LIBS in situ as a suitable quantitative analytical technique to detect the presence of boron in historical enamels even in very small quantities was assessed. Quantitative information on historical Spanish enamels and grisailles was obtained from calibration curves generated from the model glass samples with known boron content. The proposed procedure enables a satisfactory chemical quantitative study of historical glass materials *in situ*, regardless of their size, provenance, and chronology.

1. Introduction

Boron oxide is a common glass former. Its structural units coordinate with oxygen in triangles and tetrahedrons depending on the chemical composition of the glass, temperature, and pressure. Due to its high solubility, it is typically used together with SiO_2 in the form of borosilicate glasses. The addition of B_2O_3 to the silicate glass batch promotes its melting and reduces the viscosity and surface tension, which also assists the refining.[1] It also offers good durability and thermal shock resistance.

Borosilicate glass was discovered at the end of the 19th century in the Schott & Associates Glass Technology Laboratory in Jena when they began producing a series of new optical glasses containing boron oxide to solve the problem of chromatic aberration.[2,3] Nowadays, borosilicate glass is used in laboratory glassware, pharmaceutical glass tubing, cookware and kitchen implements, optical equipment, lighting technology, etc.

However, elevated boron levels are also known from historical glass. In the first millennium AD, some glasses probably produced in Asia Minor had ~1 wt % of B_2O_3 correlated with Li_2O, which could be attributed to the use of salts from the thermal waters of western Turkey.[4–8] Boron was therefore an unintentional component of the raw materials. Boron was also detected in glaze ceramics produced in Longquanwu during the Liao Dynasty and in Qing Dynasty Chinese glassware from the Museum of Fine Arts, Boston,[9] and the earliest reference to the use of borax in glass dates back to the Sung dynasty in China. In his book "Zhufanzhi" (1225), Zhao Rukuo described that the Arabs used borax in glass to withstand the most extreme temperatures and prevent cracking.[3] In Europe, borax appeared as a raw material for glass in the Bolognese manuscript (15th century) and Darduin's manuscript (16th–17th century).[10] Even their use in glass was more limited, the addition of borax in enamel and glazes was common since the 17th century in Asia (China, Japan) and Europe.[11,12]

Borax ($Na_2.xLi_xB_4O_7.10H_2O$), as the raw material of boron, has been used in enamels thanks to its highly effective fluxing and fluidifying properties that permit fixing the colored enamel to the glass surface at a relatively low temperature without deforming the support glass. Beltrán et al.[13,14] analysed replica enamels produced with the historical raw materials found in the Rigalt i Granell workshop and demonstrated that the original enamels had B_2O_3 contents between 4 and 21 wt %. In another work, Beltrán et al.[15] analysed enamelled glasses produced during the 19th and 20th centuries and detected lower concentrations of B_2O_3 (0–17 wt %), which were attributed to

[a] *Instituto de Química Física Blas Cabrera (IQF), CSIC, c/ Serrano 119, 28006 Madrid (Spain)*
[b] *Facultad de Ciencias Químicas, Universidad Complutense de Madrid, Pl. de las Ciencias, 2, 28040 Madrid (Spain)*
[c] *Instituto de Cerámica y Vidrio (ICV), CSIC. c/ Kelsen 5. Campus de Cantoblanco. 28049 Madrid (Spain)*
[d] *IRAMAT-Centre Ernest-Babelon, UMR 7065 CNRS, 3D rue de la Férollerie, 45071 Orléans (France)*
[e] *Physics Department and Barcelona Research Centre in Multiscale Science and Engineering, Universitat Politècnica de Catalunya, Campus Diagonal Besòs, Av. Eduard Maristany, 10–14 08019 Barcelona (Spain)*
[f] *UI VICARTE Vidro e Cerâmica para as Artes, NOVA School of Science and Technology, Universidade Nova de Lisboa, Campus da Caparica 2829–516 Caparica (Portugal)*

Correspondence: *Mohamed Oujja, Instituto de Química Física Blas Cabrera (IQF), CSIC, c/ Serrano 119, 28006 Madrid (Spain).*
Email: m.oujja@csic.es

Teresa Palomar, Instituto de Cerámica y Vidrio (ICV), CSIC. c/ Kelsen 5. Campus de Cantoblanco. 28049 Madrid (Spain).
Email: t.palomar@fct.unl.pt

Research Article
doi.org/10.1002/cmtd.202400057
Chemistry Europe
European Chemical Societies Publishing

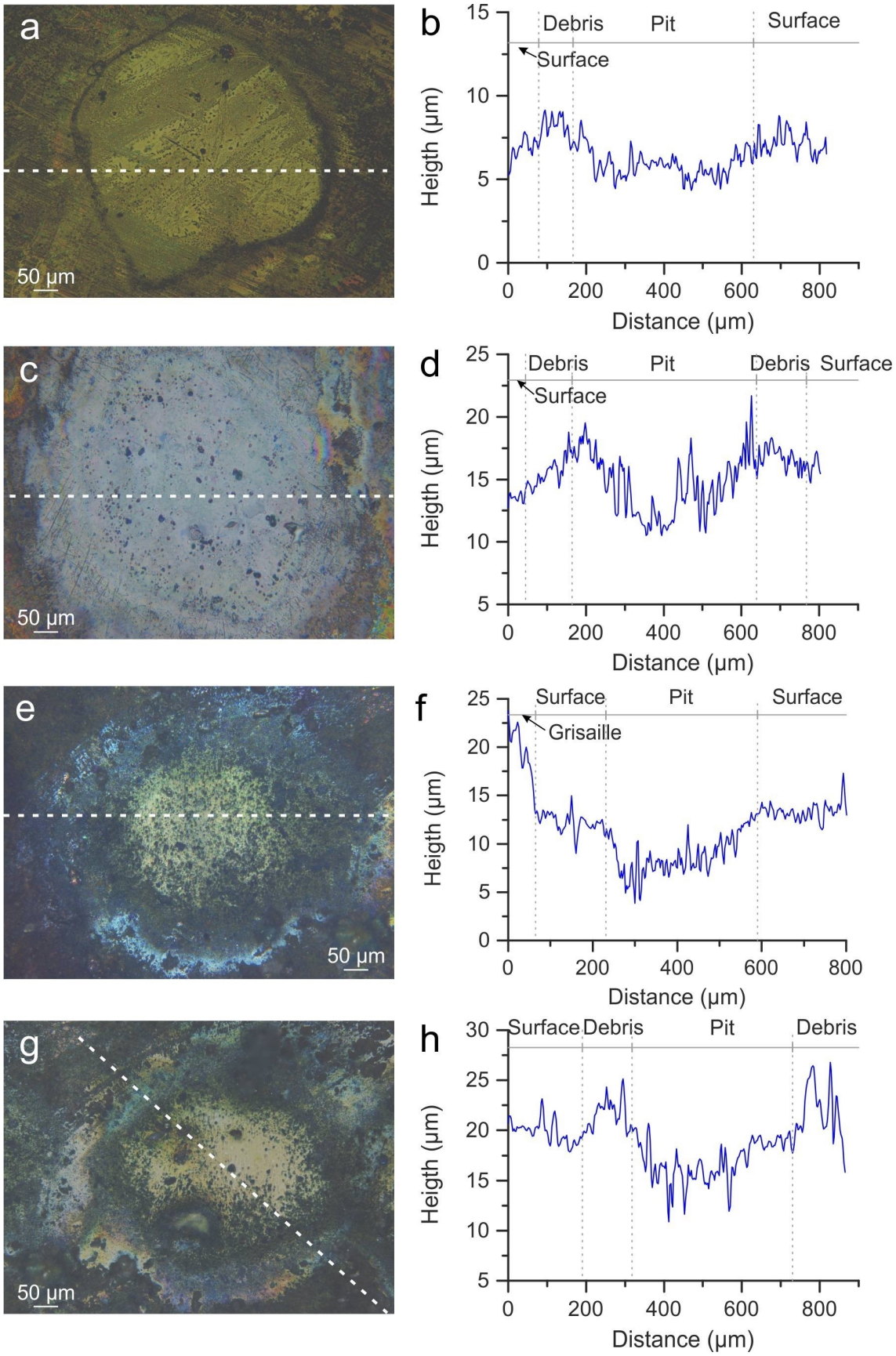

Figure 1. Optical profiles on the pits produced by LIBS: a–b) E3-yellow, c–d) E131-blue, e–f) BC3B-purple, and g-h) BC3B-blue. The white dashed line indicates the area considered for the surface roughness representation.

Research Article
doi.org/10.1002/cmtd.202400057
Chemistry Europe
European Chemical Societies Publishing

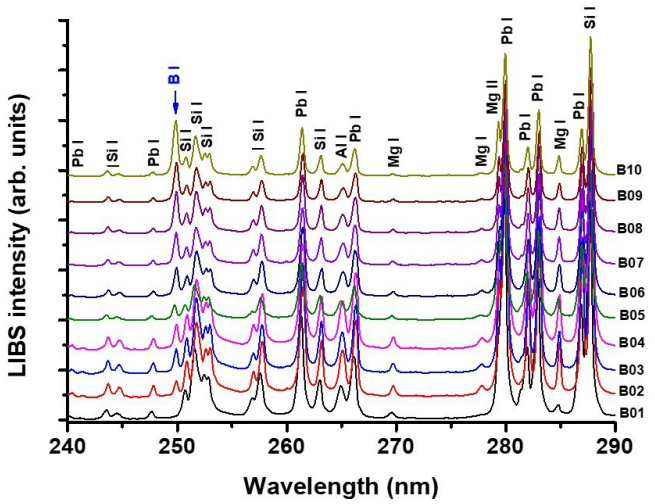

Figure 2. LIB spectra of reference glass samples in the 240–290 nm wavelength range. The LIB spectra correspond to a single laser pulse. The time delay and gate width were 200 ns and 3 μs, respectively. The assignment of the line emissions is done using the NIST database.[48] The blue arrow indicates the boron emission at 249,67 nm.

the leaching of boron during the alteration of the glass. Borax was also occasionally used in historical grisailles.[16] Pradell et al.[17] identified boron in grisailles from the Cathedral of Segovia (Spain) from the 17th century onwards, and Machado et al.[18] identified boron in two 20th-century samples from Germany (Glasmalerei Otto Peters atelier) and Sweden (Uppsala Cathedral). In the latter case, the boron was associated with a high zinc oxide content and may indicate that an enamel made from lead–zinc borosilicate glass was used as the base glass instead of lead-silica glass.[14]

Analysing the chemical composition of historical glasses, especially those containing boron, is often a challenge and related studies are very scarce. Ma et al.[9] analysed a set of Qing Dynasty glass vessels from the Bristol Museum and Art Gallery by Electron Microprobe Analysis (EPMA) and detected high content of B_2O_3 in two samples from the 17th century. Kunicki-Goldfinger et al.[19] also analysed several glasses with EPMA and detected contents of B_2O_3 up to 4 wt % in 17th-century glass vessels, and up to 2.5 wt % in central European potassium glasses from the post-medieval and baroque periods. In the case of surface decoration, Van der Snickt et al.[20] attributed a high concentration of boron to 20th-century enamels based on the high content of sodium and the absence of potassium detected by EMPA, which ascribed to the use of borax. Devulder et al.[21] analysed the boron content and their isotope ratio in Roman glass fragments with a quadrupole ICP-MS and Multi-collector Inductively Coupled Plasma Mass Spectrometry (MC-ICP-MS) by dissolving the glass samples. Beltrán et al.[10–12] and Pradell et al. [14] used the LA-ICP-MS on Modern and Contemporary enamels and grisailles in stained-glass windows detecting B_2O_3 up to 20 wt %. Machado et al.[15] used Laser Induced Breakdown Spectroscopy (LIBS) to identify the presence of boron in historical grisailles.

Most archaeological glasses are fragments[22] that can either be sampled or are small enough to be analysed in the

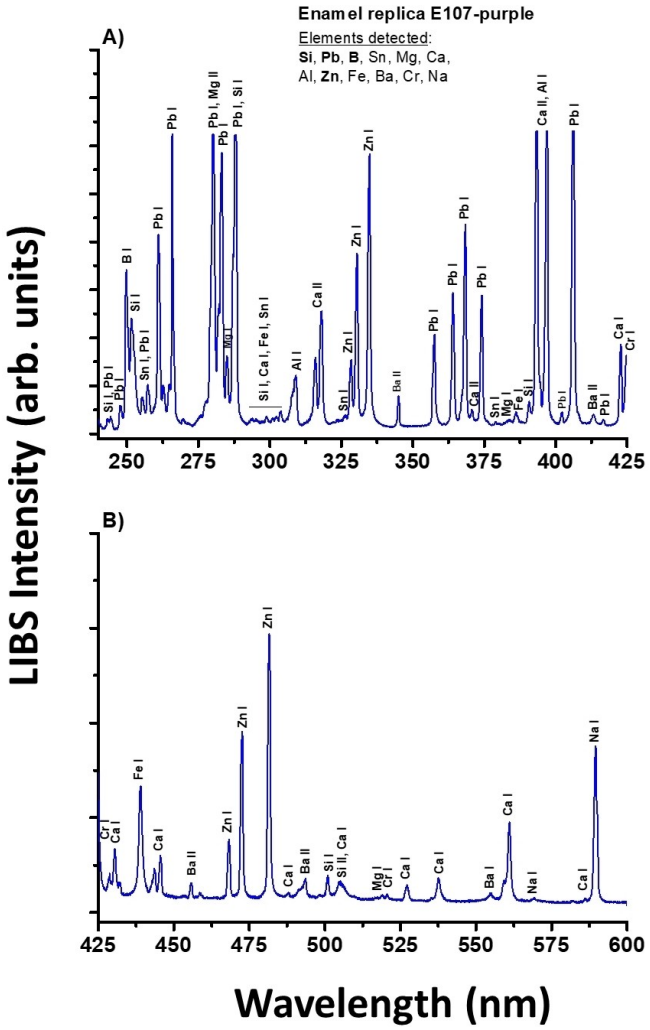

Figure 3. LIB spectra of the enamel replica E107-purple in the spectral ranges, A) 240–425 nm and B) 425–600 nm. It corresponds to a single laser pulse. The time delay and gate width were 200 ns and 3 μs, respectively. The assignment of the line emissions is done using the NIST database.[48] The main detected components are indicated in bold.

laboratory. However, modern and contemporary glasses are frequently completely preserved objects from which taking a sample is almost impossible. The most common analytical techniques for archaeological and historical glasses are X-ray fluorescence (XRF), Scanning Electron Microscopy - Energy Dispersive X-ray spectroscopy (SEM-EDS)[22] and electron microprobe wavelength dispersive X-ray spectrometry (EPMA).[9,19,20] All these three methods collect the X-rays emitted by the elements present in the sample. SEM-EDS detection limits are typically in the order of 0.1 wt % and as a result, only major elements can be measured in glass. XRF penetrates a few μm at low energies and several mm at high energies allowing better detection limits (10-50 ppm) depending on the element, beam collimator size, and detector type.[23] EPMA has better (lower) detection limits than SEM-EDS, but light elements such as boron nonetheless pose a problem. Hence, none of these techniques can reliably measure the boron contents in glass. Raman micro-spectroscopy has also demonstrated its potential

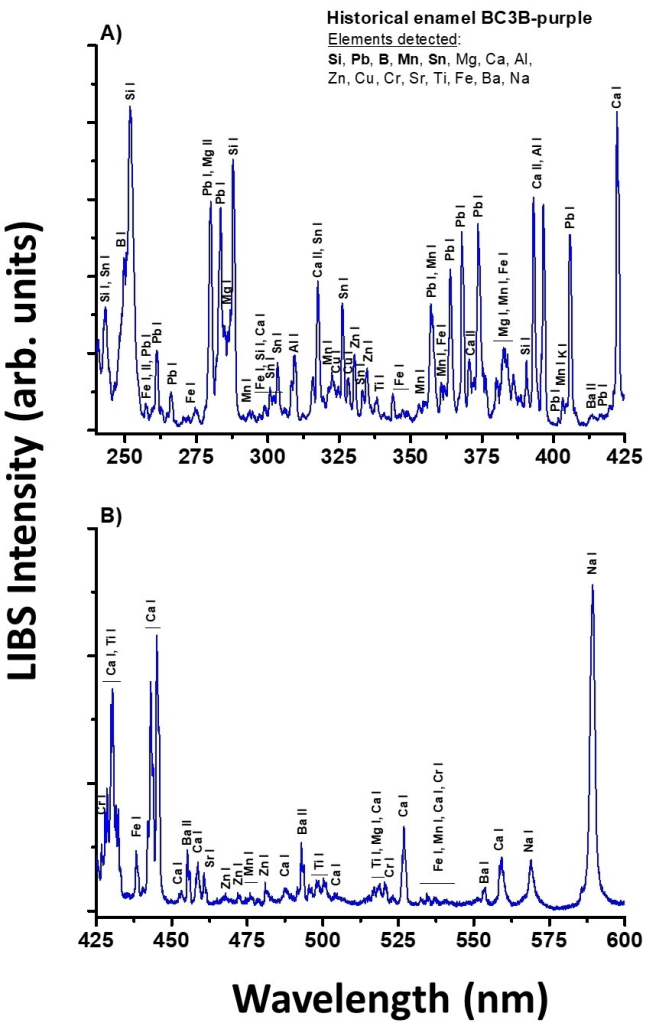

Figure 4. LIB spectrum of the historical enamel sample BC3B-purple in the spectral ranges, A) 240–425 nm and B) 425–600 nm.. The LIB spectrum corresponds to a single laser pulse. The time delay and gate width were 200 ns and 3 μs, respectively. The assignment of the line emissions is done using the NIST database.[48] The main detected components are indicated in bold.

for the non-invasive analysis of enameled glass objects in the laboratory or *in situ* with mobile instruments.[24,25]

The proton-induced X-ray/γ-ray emission (PIXE/PIGE) is a multi-elemental analysis that is suitable for major, minor, and trace elements. It is characterized by high sensitivity and speed in obtaining analytical data, the absence of any pre-treatment, preparation, and handling of samples, and their non-destructive nature.[26] Compared to XRF, the detection limits offered by PIXE are better by one order of magnitude.[27] The sample is normally placed in a chamber inside the acceleration vacuum for direct excitation or placed directly in the external beam under atmospheric pressure for surface analysis but, in case of altered samples, the analytical error increases. This technique allows the detection of boron,[28] but not the *in situ* measurements because it involves a nuclear accelerator, which is a large infrastructure.

The inductively coupled plasma methods (ICP-OES and ICP-MS) enable the determination of a wide range of elements (major, minor, and trace elements), high selectivity including low Z elements such as boron and low detection limits even at ppb level. The disadvantage is that a smaller amount of sample needs to be removed for analysis as most devices require the digestion of the glass into a solution, which is not always possible with historical glass samples. LA-ICP-MS, on the other hand, uses a laser beam with a diameter of 20–100 μm to remove a sample from the glass surface. The ablated material is then atomized and ionized in the plasma and analysed in the mass spectrometer. It can therefore be considered a minimally (micro−) destructive technique that does not require sample preparation.[23] However, high vacuum conditions are needed, making the analysis of large or voluminous pieces difficult and *in situ* analyses are simply impossible.

Among the laser-based techniques to analyse glasses the most used is LIBS, similar to LA-ICP-MS. LA-ICP-MS transports the nanoparticles ablated to the ICP-MS to be ionized and detected by mass-to-charge ratio, while LIBS uses a laser pulse to create a micro-plasma and excite species from the sample. When the excited electrons return to natural ground states, they emit light that is simultaneously detected.[23] This method is a popular elemental analytical technique because of its micro-destructive nature, speed of detection, no need for prior sample preparation, and inexpensive hardware. It can be used to investigate a wide range of materials in solid, liquid, or gaseous phases.[29,30] LIBS has demonstrated its potential in archaeology and cultural heritage conservation due to its advantageous characteristics for surface and in-depth profiling analysis.[31] Therefore, it is not surprising that LIBS is used for a wide variety of applications, such as glasses,[32–39] geomaterial analysis,[40] environmental monitoring,[41] forensics,[42] biological identification,[43] and even characterization of fossils[44] and works of art.[45]

Most of the analytical techniques cited previously need small-size objects or sampling, which is not recommended for cultural heritage objects. For this reason, this work aims to develop a protocol based on calibration curves to determine and quantify the boron content in paintings on historical stained-glass windows using the micro-destructive technique LIBS. This protocol will be useful to be applied *in situ* in museums avoiding sampling and transporting the historical objects to the laboratory.

2. Materials and Methods

A set of ten glasses with different boron contents were prepared to serve as reference samples. First, a frit was prepared with PbO: SiO_2 (3:1) and then mixed with B_2O_3 in different proportions to obtain the ten reference glasses (Table 1).

Research Article
doi.org/10.1002/cmtd.202400057
Chemistry Europe
European Chemical Societies Publishing

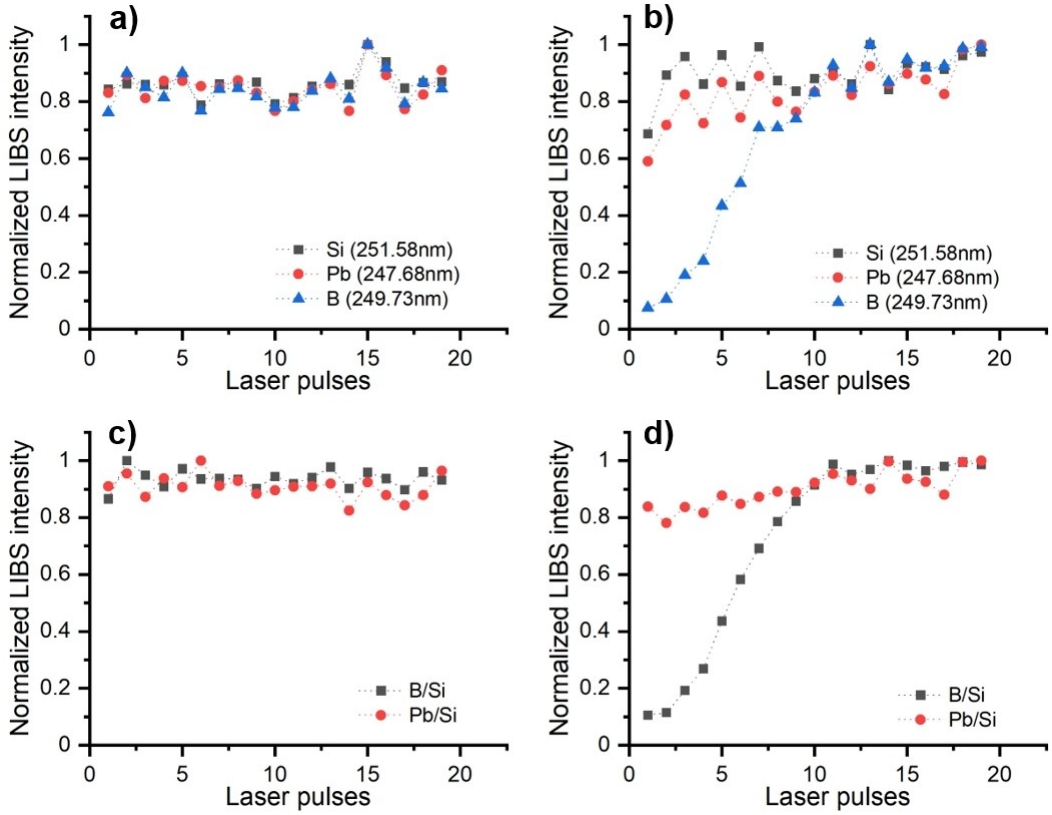

Figure 5. LIBS stratigraphic analysis of the sample (a) E131-blue – enamel replica and (b) EN1 C-yellow - historic enamel based on in-depth profiling of Si emission at 251.58 nm, Pb emission at 247.68 nm and B emission at 249.73 nm. Ratio values for Pb/Si and B/Si show high stability in the composition of the enamel replicas ((c) E131-blue), however, the historic enamel ((d) EN1 C-yellow) indicates a significant increase in the boron content from the surface to the core samples.

Table 1. Theoretical composition and preparation conditions of the ten glass references. For all samples, the preparation time was 2 hours.

Sample	Theoretical composition (wt%)		Melting Temperature (°C)	Annealing Temperature (°C)
	B_2O_3	$SiO_2 + PbO$		
B01	0	100	800	400
B02	0.25	99.75	800	400
B03	0.50	99.5	800	400
B04	0.75	99.25	800	400
B05	1	99	800	400
B06	5	95	700	400
B07	10	90	700	300
B08	15	85	700	300
B09	20	80	600	250
B10	30	70	600	250

2.1. Historical Samples

Two sets of samples were analysed. The first set consists of enamel replicas made by J.M. Bonet Vitralls S.L. based on materials of historical enamels from the Rigalt, Granell & cia workshop[14] and the second includes historical pieces (enamels and grisailles) of Catalan Modernist stained-glass windows.[15]

2.2. Analytical Methods

The reference glasses, enamel replicas and historical samples were analysed by LA-ICP-MS, optical profilometry and LIBS.

LA-ICP-MS has been carried out at IRAMAT-CEB in Orléans (France). The analyses were done using a Resonetics M50E excimer laser (ArF, 193 nm) equipped with a S155 ablation cell and a Thermo Fisher Scientific ELEMENT XR mass spectrometer system. The ablations were typically carried out with a 5 mJ

Research Article
doi.org/10.1002/cmtd.202400057
Chemistry Europe
European Chemical Societies Publishing

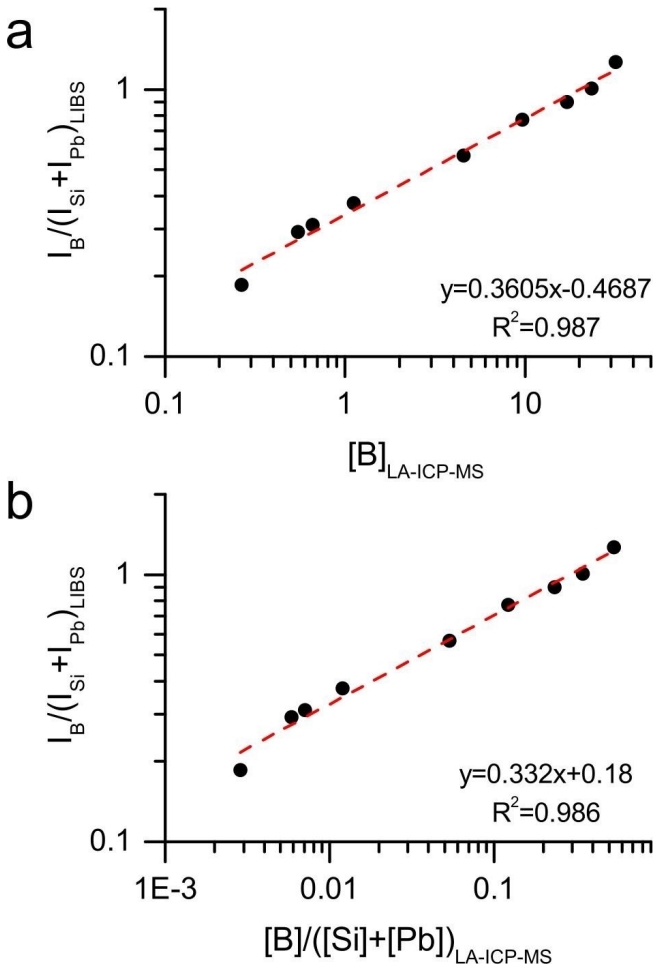

Figure 6. Calibration curves obtained using, (a) the ratio of the relative intensities of boron and silicon with lead (I_B / ($I_{Si}+I_{Pb}$)) determined by LIBS as a function of the boron content measured by LA-ICP-MS (first approach), and (b) the ratio of the relative intensities of boron and silicon with lead determined by LIBS, as a function of the boron content (unknown) represented as a function of the content of silicon and lead determined using LA-ICP-MS (second approach).

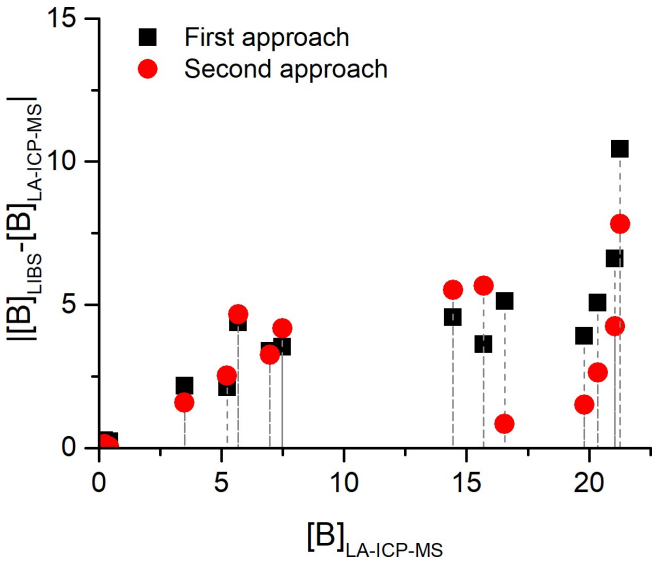

Figure 7. Representation of the obtained error values of LIBS analysis as a function of the boron content determined using LA-ICP-MS.

energy at 10 Hz pulse frequency in spot-mode and a beam diameter of 100 μm for the base glass. The enamels were typically analysed on the surface due to insufficient thickness with a beam diameter of 50 μm that was occasionally reduced down to 25 μm when saturation of the signal caused by high concentrations of transition metals occurred. A pre-ablation time of either 10 s or 20 s depending on the thickness of the sample was followed by 30 s signal acquisition, resulting in 10 mass scans. The ablated material is transported to the plasma torch by an argon/helium flow at an approximate rate of 1 L/min for Ar and 0.65 L/min for He. The ion signals in counts-per-second are recorded for 58 isotopes (from Li to U). Standard Reference Material (NIST SRM610) as well as Corning glasses B, C, and D and APL1 (in-house standard glass) were used for external calibration, while ^{28}Si was used as internal standard. Quantitative concentrations were calculated based on the procedures described by Gratuze.[46] Precision and accuracy are reflected in the repeated measurements of reference glasses Corning A and NIST SRM612.

The samples surfaces were observed in a Zeta Instruments optical profilometer model Zeta-20 used as an optical microscope.

LIBS analysis was carried out, at ambient atmospheric conditions, on the surface and in-depth (stratigraphic study) of the considered glass samples using laser excitation at 266 nm (4th harmonic of a Q-switched Nd: YAG laser (Lotis TII, LS-2147), 15 ns pulses, 1 Hz repetition rate). LIB spectra were recorded using a 0.2 m Czerny-Turner spectrograph (Andor, Shamrock Kymera-193i-A) equipped with a grating of 1800 grooves/mm (blazed at 265 nm) and coupled to a time-gated intensified charge-coupled device (ICCD) camera (Andor Technology, iStar CCD 334, 1024x1024 active pixels, 13 μm x 13 μm pixel). The ICCD detector is synchronized with the Q-Switch output electrical signal that triggers the laser pulse. The laser beam was directed to the surface of the samples by the use of mirrors at an incidence angle of 45°. Focusing with a 10 cm focal length lens allowed fluences in the range of 5–9 J cm^{-2} to be achieved. The shot-to-shot laser energy fluctuation was less than 10%. LIB spectra were recorded in the 240–600 nm wavelength range using a step and glow mode at intervals of 30 nm. For the stratigraphic analysis, the spectra were recorded by applying several laser pulses in the same area of the samples at 30 nm wavelength intervals centered at 285, 325, 360, 400 and 500 nm. The spectra were acquired at a 0.17 nm resolution with a gate delay and width of 200 ns and 3 μs, respectively. For higher wavelengths, a cut-off filter at 300 nm was placed in front of the entrance window of the spectrograph to reduce the scattered laser light and to avoid second-order diffractions. Each LIB spectrum resulted from a single signal acquisition as it provides good signal/noise ratios.

2.3. Samples Preparation

For the LIBS technique no sample preparation is needed prior to their analysis, in fact, it is one of the advantages of this technique. Using the LA-ICP-MS technique, the reference glasses and enamel replicas were analyzed on unprepared samples. In contrast, the historical glass samples were mounted in resin and analyzed in cross-section after polishing processes.

3. Results and Discussion

3.1. LA-ICP-MS

The LA-ICP-MS analyses of the reference glasses revealed a composition that deviates somewhat from the nominal chemical composition theoretically calculated (Table 1 and Table 2), probably because of the liquid immiscibility of the compounds at higher contents of boron.[47] The relatively high alumina content was attributed to the use of porcelain crucibles during melting.

The enamel replicas showed a high content of SiO_2, B_2O_3, ZnO and PbO (Table 2). SiO_2 was the former of the glass network together with B_2O_3 and PbO that decreased the glass transition temperature (T_g). This enables the enamels to be fixed to the surface of the glass without any deformation effect. The presence of ZnO also lowers the melting temperature, while the coefficient of thermal expansion increases, thereby increasing the resistance to thermal shock. The replicas have 16–21 wt% B_2O_3, 40-53 wt% PbO and, 11–14 wt% ZnO except for sample E3-yellow that has lower B_2O_3 (7 wt%) and ZnO (0.1 wt%) but higher SiO_2 (~30 wt%) (Table 2). The different coloration of the enamels is due to minor elements such as MnO, Cr_2O_3, CuO, or CoO. The MnO is related to purple and brown, Cr_2O_3 was detected in the brownish enamels, while CuO and CoO are responsible for blue (Table 2).

Compared to the enamel replicas, the historical pieces have lower B_2O_3 (3-15 wt%) content (Table 2). A high concentration of ZnO was observed only in two of the samples, BC3B-blue and EN1 C-yellow. These differences could to a certain extent be the result of surface alterations in which the water from rain and condensation leached the boron.[15] Regarding the chromophores, the historical glasses have relatively high concentrations of MnO, Fe_2O_3, Cr_2O_3, CuO, and CoO.

Table 2. Chemical composition of the different glass-based samples determined by LA-ICP-MS.

		Chemical composition (wt%)												
	Sample	B_2O_3	Na_2O	Al_2O_3	SiO_2	CaO	Cr_2O_3	MnO	Fe_2O_3	CoO	CuO	ZnO	SnO_2	PbO
Reference glasses	B01	0.0	0.0	7.4	21.3	0.0	0.0	0.0	0.0	0.0	0.0	0.0	0.0	71.2
	B02	0.3	0.0	5.8	23.5	0.5	0.0	0.0	0.0	0.0	0.0	0.0	0.0	69.4
	B03	0.5	0.0	5.2	23.3	0.6	0.0	0.0	0.0	0.0	0.0	0.0	0.0	70.0
	B04	0.7	0.1	5.3	22.4	0.5	0.0	0.0	0.0	0.0	0.0	0.0	0.0	70.8
	B05	1.1	0.0	5.3	22.7	0.6	0.0	0.0	0.0	0.0	0.0	0.0	0.0	70.1
	B06	4.5	0.0	9.7	24.3	0.6	0.0	0.0	0.1	0.0	0.0	0.0	0.0	60.4
	B07	9.6	0.0	10.3	23.6	0.5	0.0	0.0	0.1	0.0	0.0	0.0	0.0	55.4
	B08	17.1	0.0	9.3	26.2	0.2	0.0	0.0	0.1	0.0	0.0	0.0	0.0	46.8
	B09	23.3	0.0	8.6	23.7	0.1	0.0	0.0	0.1	0.0	0.0	0.0	0.0	43.8
	B10	31.8	0.0	8.0	22.1	0.2	0.0	0.0	0.0	0.0	0.0	0.0	0.0	37.4
Enamel replicas[14]	E3-yellow	7.0	5.1	0.3	30.4	2.6	1.2	0.0	0.1	0.0	0.0	0.1	0.0	53.0
	E14-purple	21.1	2.1	0.3	8.6	0.9	0.0	0.0	0.1	0.0	0.0	11.2	1. 8	53.2
	E23-red	16.5	0.8	0.3	9.3	0.5	0.0	0.0	0.0	0.0	0.0	14.0	7.6	40.8
	E107-purple	19.8	0.9	0.2	8.9	0.6	0.0	0.0	0.1	0.0	0.0	13.8	2.6	52.6
	E119-yellow	20.3	1.1	0.2	8.2	0.5	0.5	0.0	0.1	0.0	0.0	13.9	1.4	53.4
	E131-blue	21.3	1.5	0.5	9.3	0.7	0.0	0.0	0.0	0.1	0.0	12.9	1.3	52.0
Historical pieces[15]	BC3B-blue	5.2	4.9	3.6	28.3	1.2	1.8	0.4	1.8	1.6	0.0	8.0	0.0	42.2
	BC3B-purple	5.7	6.9	1.1	29.2	1.9	0.1	1.4	4.9	0.1	0.0	0.9	5.6	40.2
	BC3B-brown	0.2	12.5	1.3	53.2	6.1	0.0	1.4	5.2	0.0	0.0	0.1	0.0	18.9
	BC3 C-green	7.5	6.3	1.9	26.5	7.1	2.9	0.1	0.4	1.5	1.6	2.2	0.0	40.5
	EN1 A-green	15.7	1.4	0.8	15.8	0.8	0.2	0.0	0.1	0.0	1.6	1.9	0.0	61.3
	EN1 A-grisaille	0.4	10.3	0.3	58.1	9.8	0.0	1.6	9.9	0.0	1.1	0.9	0.0	6.8
	EN1 C-yellow	14.5	1.5	0.5	15.0	1.0	1.3	0.0	0.0	0.0	0.0	7.4	0.0	58.4
	PG2 C-purple	3.5	6.8	0.7	41.6	5.8	0.0	0.9	3.4	0.0	0.0	0.2	5.9	27.9

Research Article
doi.org/10.1002/cmtd.202400057
Chemistry Europe
European Chemical Societies Publishing

Table 3. Summary of the boron content determined using the calibration curves from the two considered approaches based on LA-ICP-MS and LIBS measurements. * without LA-ICP-MS.

Sample	Considered laser pulses for LIBS analysis	[B] by LA-ICP-MS	LIBS intensities $I_B/(I_{Si}+I_{Pb})$	First approach $(I_B/(I_{Si}+I_{Pb}))_{LIBS}$ vs $[B]_{LA\text{-}ICP\text{-}MS}$		Second approach $(I_B/(I_{Si}+I_{Pb}))_{LIBS}$ vs $[B]/([Si]+[Pb])_{LA\text{-}ICP\text{-}MS}$	
				Calculated [B] (wt%)	Deviation	Calculated [B] (wt%)	Deviation
E3-yellow	2–20	7.0	0.54	3.6	3.4	3.7	3.3
E14-purple	2–20	21.1	1.12	27.7	6.6	25.3	4.3
E23-red	2–20	16.5	1.03	21.7	5.1	15.7	0.8
E107-purple	2–20	19.8	1.06	23.7	3.9	21.3	1.5
E119-yellow	2–20	20.3	1.09	25.4	5.1	23.0	2.6
E131-blue	2–20	21.3	1.18	31.7	10.4	29.1	7.8
BC3B-blue	6–20	5.2	0.51	3.1	2.1	2.7	2.5
BC3B-purple	7–20	5.7	0.37	1.3	4.4	1.0	4.7
BC3B-brown	11–20	0.2	0.26	0.5	0.3	0.4	0.1
BC3 C-green	7–20	7.5	0.56	3.9	3.5	3.3	4.2
EN1 A-green	14–20	15.7	0.99	19.3	3.6	21.4	5.7
EN1 A-grisaille	7–20	0.4	0.29	0.7	0.2	0.5	0.1
EN1 C-yellow	11–20	14.5	0.98	19.0	4.6	20.0	5.5
PG2 C-purple	9–20	3.5	0.64	5.7	2.2	5.1	1.6
BC2 C-blue	16–20	*	0.70	7.5	–	*	–
BC3B-grisaille	9–20	*	0.17	0.2	–	*	–
EN1 C-grisaille	6–20	*	0.16	0.1	–	*	–
PG2B-blue	5–20	*	0.26	0.4	–	*	–
PG2B-brown	5–20	*	0.25	0.4	–	*	–
PG2B-grisaille	11–20	*	0.25	0.4	–	*	–

3.2. LIBS

3.2.1. Laser Ablation Effects

The laser irradiation induces the ablation of the samples surface creating a pit of Ø ~350 μm with the material ejected accumulating around its border (Figure 1 a, c, e and g). It is also possible to observe iridescence effects due to the material vaporization and deposition in the crater surroundings without ruling out the melting effects producing the optical phenomenon of light dispersion. In the enamel replicas, a different behaviour was observed as a function of the chemical composition (Figure 1 a–d). In sample E3-yellow, with a higher sodium content, a homogeneous pit was created with a small hole depth (~2 μm) (Figure 1 b). In the samples with a higher boron content such as E131-blue, the pits appeared irregular with an aspect of melted material (Figure 1 **c**). This behaviour is consistent with the glass transition temperature (T_g) of the materials, where higher content lowers the T_g and the heating generated by the laser can therefore cause the material to melt. Additionally, the pits were deeper, and more debris accumulated around them (Figure 1 d).

In the historical pieces, the diameter of the laser spot was ~350 μm with a depth of ~7 μm (Figure 1 e–h). Iridescence effects were likewise observed in the accumulated material around the pit. In contrast to the enamel replicas, the hole is very irregular, which is probably due to the original heterogeneity of the historical enamel. This, in turn, is influenced by the painter's artistic method, the presence of a very thin layer of grisaille with metallic grains, and the surface of the base glass. The morphology of the laser spot is similar to sample E3-yellow (Figure 1 a–b), since they have a high SiO_2 content (Table 2), and, therefore, the Tg is higher.

3.2.2. Qualitative Analysis

LIB spectra showed the elemental composition of the investigated samples according to the emission lines of the major and minor components, including the chromophores which are responsible for their colour. The reference glasses exhibit a small number of emission lines due to the limited number of elements used as raw materials in their preparation (Table 1). Emission peaks of Si, Pb, B, Al, and Mg are evident (Figure 2). The emission of B at 249.73 nm (indicated with a blue arrow in Figure 2) showed a progressive increase of its intensity in accordance with the increase of boron concentration of the different prepared samples (as observed by LA-ICP-MS, Table 2).

The spectra of the enamel replicas, for example, E107-purple (Figure 3), contained lines of Si, B, and Pb like the reference material, but also of other elements such as Zn, Ca, Mg, Al, Na and Ba related to the presence of stabilizers or Sn, Fe and Cr

due to chromophores and opacifiers. The high intensity of the main elements (Si, Pb, B, Zn) corresponds to their highest concentration, as determined by LA-ICP-MS (Table 2).

The LIB spectra of the historical pieces are richer in line emissions because they contain a higher number of elements in their composition (Figure 4). In addition to the main elements B, Pb, Mn, Sn, and Si, elements such as Mg, Ca, Al, Zn, Sr, Ti, Fe, Ba and Na appeared as minor ones. Fe, Cu, Cr, and Mn can be assigned to the presence of chromophores or be part of the thin layer of grisaille.[16]

The comparison with data from LA-ICP-MS (Table 2) reveals that LIBS can detect the presence of most elements identified by LA-ICP-MS without prior sample preparation.

3.2.3. Boron Degradation Profiling

To study the effects of corrosion on the surface composition of the glass samples, several consecutive laser pulses were applied on the same spot of the sample. LIB spectra were recorded after each impact up to 20 pulses and provided useful information about possible changes in the chemical composition. The enamel replicas, such as E131-blue (Figure 5 a and c), show the same chemical composition of the main elements (Si, B, and Pb) from the surface to the core. This means that the chemical composition of the material remains stable and unaltered. The enamel replicas have been never exposed to the external environment and are therefore perfectly preserved.[14] In contrast, the historical enamels (e.g. EN1 C-yellow) show a loss of boron in the outer layers as a consequence of its solubility in the surrounding water[49] (Figure 5 b), without ruling out the contribution of its surface loss at the firing temperature during enamel production.[12] The ratio between lead and silica shows that the lead has also suffered a slight loss (Figure 5 d), probably because the element has a larger ionic radius and its leakage is not favoured.

These examples demonstrate the importance of stratigraphic analyses of historical glass before their analysis to determine if the surface is altered. Stratigraphic study is therefore of fundamental importance for the development of analytical methodologies because the presence of alteration layers or a leached surface can drastically modify the core chemical composition, making it impossible to relate the results of non-destructive analyses of the surface to the glass core.

3.2.4. Determination of Calibration Curves

To perform quantitative LIBS analysis of boron in unknown samples, we constructed calibration curves using the boron emissions from the reference samples whose composition had been established by LA-ICP-MS (listed in Table 2). For this purpose, the line intensities corresponding to boron in the reference samples at 249.73 nm were normalized to the Si I and Pb I emissions at 251.58 and 247.68 nm, respectively, which were used as an internal standard. This procedure is a common approach in LIBS analysis and serves to minimize the fluctuations that can arise from matrix effects and laser instability.[34,38,50] On the other hand, the peaks selected for the calibration curves (B at 249.73 nm, Si at 251.58 nm, and Pb at 247.68 nm) were nearer in the LIBS spectra to avoid alterations in the emission intensities due to possible effects caused by the detection system (spectrograph and ICCD detector).

Two approaches for the determination of calibration curves were evaluated. In the first, the ratio of the corresponding relative intensities of boron and silicon with lead, determined by LIBS measurements was represented as a function of the boron content (in wt%) measured by LA-ICP-MS (Table 2). Figure 6 a, presents the calibration curve showing a fairly good linearity, with correlation coefficients near unity (0.98). For better visualization of the calibration curve, the axes were represented in logarithmic mode (Figure 6). In the second approach, the ratio of the relative intensities of boron and silicon with lead obtained by LIBS was represented as a function of the ratio between the amount of boron and silicon with lead obtained by LA-ICP-MS to minimize the possible errors in the determination of the amount of boron (Figure 6 b). In this case, the calibration line showed a similar regression value as the previous approach ($R^2 > 0.98$). For this second approach, the determination of the amount of the main elements, silicon and lead, of the glass matrix is necessary and requires the use of an additional quantitative analytical technique, such as LA-ICP-MS, XRF, and SEM-EDS.

From the minimum measurable relative intensity of B to Si and Pb lines, it is estimated that the calibration performed herein allows the reliable detection of boron contents even at very low quantities. This indicates that LIBS is a very sensitive technique for detecting the presence of boron in historical glass objects.

3.3. Validation Tests and Case Studies

To validate the two approaches, they were applied to estimate the boron content of enamel replicas and historical pieces. Table 3 summarises the concentrations of boron determined in each case. The values obtained for the different samples studied using LIBS (enamel replicas and historical pieces) are in very good agreement with those obtained by LA-ICP-MS.

The error in the calculations of the boron content tends to be higher when using the first approach than the second one (Table 3), since in the latter the contents of silicon and lead were taken into account for estimating the boron content. The errors increase at higher boron concentrations (Figure 7). The first approach presents an average error of ± 4.0 wt%, it remains always < 7 wt%, except for the sample E131-blue (error = 10.4 wt%), which is the sample with the highest content of boron (Table 2). A similar behaviour was observed using the second approach. The average error is ± 3.2 wt%, being < 6.0 wt% except for the sample E131-blue in which it was measured 29.1 wt% instead of 21.3 wt% (Table 3).

Some areas of the historical pieces were analysed by LIBS but not by LA-ICP-MS (Table 3). The blue area of BC2 C-blue showed a concentration of boron similar to some of the other

enamels (e.g. PG2 C-purple). The grisailles in BC3B, EN1 C and PG2B presented boron contents below 0.5 wt%. This low concentration is common in historical grisailles that use lead as flux instead of boron.[16] Finally, the enamels in PG2B blue and brown areas showed a similar content of boron to the PG2B-grisaille (~0.4 wt%), which probably corresponded to the grisaille layer that covered the sample to shade the light.

4. Conclusions

This work validates the use of LIBS for qualitative and quantitative determination of boron content in enamels and historical glass samples. For this purpose, a selection of reference glasses with a well-known boron content was used to create the calibration curves based on two approaches (see section 3.2.4). The most representative elements of the paintings on glass samples (Si, Ca, Na, K, and Pb) and some chromophores (Mn, Cr, Fe and Cu) were identified by the LIBS technique.

By applying successive laser pulses on the same area of the samples studied (enamel replicas and historical pieces), LIBS provided information on the possible changes in their chemical composition induced by corrosion effects. In this way, it was possible to carry out a correct quantitative analysis of the different components without interferences from the corrosion layers. However, this technique still has limitations when dealing with severely corroded or deteriorated samples, which may affect the data accuracy.

The quantitative boron analyses in the enamel replicas and historical pieces by LIBS were validated by comparison with the results from LA-ICP-MS, using calibration-based approaches relying on reference laboratory glasses with well-known boron content. The calibration curves showed a good linearity with low deviation. The first approach referred to LIBS and LA-ICP-MS results, but the second requires the use of another quantitative analytical technique (LA-ICP-MS, XRF, SEM-EDX, etc.) to determine the amounts of the main elements of the painting material (in this case silicon and lead) to normalise the calculated amount of boron.

The present study demonstrates that LIBS is a useful, promising, and alternative technique for investigating boron content in historical glass samples, especially those with corrosion layers, and more generally for the *in situ* investigation of non-destructible cultural heritage materials. The speed of analysis of this technique facilitates the analysis of samples in the field, at excavation sites, or in museums, galleries, or cultural institutions. Also, the availability of portable LIBS devices alone or in combination with other analytical techniques such as XRF, enables the analysis on-site, without sample preparation and size limits of a huge number of component elements of cultural heritage objects.

Acknowledgements

This research has been funded by the Fundação de Ciência e Tecnologia from Portugal (project ref. UIDB/EAT/00729/2020, UIDP/00729/2020, 2023.05135.RESTART, and researcher grant CEECIND/02249/2021), the Spanish State Research Agency (AEI) through the projects PID2022-137017OB-I00/AEI/1013039/501100011033 and PID2022-137783OB-I00, the Regional Government of Madrid through the project TEC Heritage-CM (TEC-2024/TEC-39), the Generalitat de Catalunya through the Consolidated Group 2021 SGR 00343, support from CSIC Platform 'Open Heritage: Research and Society' (PTI-PAIS) and the CSIC Open Access Publication Support Initiative through its Unit of Information Resources for Research (URICI) are acknowledged. Teresa Palomar thanks MICIU for Ramón y Cajal contract (RYC2023-045699-I).

Conflict of Interests

The authors declare no conflict of interest.

Data Availability Statement

The data that support the findings of this study are available from the corresponding author upon reasonable request.

Keywords: Boron · Enamels · Grisailles · *In-situ* Analysis · Laser-Induced Breakdown Spectroscopy · Laser Ablation Inductively Coupled Plasma Mass Spectrometry

[1] J. M. Fernández Navarro, *El Vidrio. 3ª* Ed, Consejo Superior De Investigaciones Científicas. Sociedad Española De Cerámica Y Vidrio, Madrid, **2003**.
[2] R. E. Youngman, *in Encycl. Glas. Sci. Technol. Hist. Cult., Wiley* **2021**, pp. 867–878.
[3] J. Steiner, *Glas. Berichte* **1993**, *66*, 165–173.
[4] N. Schibille, *PLoS One* **2011**, *6*, e18970.
[5] M. A. Gómez-Morón, T. Palomar, L. C. Alves, P. Ortiz, M. Vilarigues, N. Schibille, *J. Archaeol. Sci.* **2021**, *129*, 105370.
[6] M. S. Tite, A. J. Shortland, N. Schibille, P. Degryse, *Archaeometry* **2016**, *58*, 57–67.
[7] J. de Juan Ares, A. Vigil-Escalera Guirado, Y. Cáceres Gutiérrez, N. Schibille, *J. Archaeol. Sci.* **2019**, *107*, 23–31.
[8] C. M. Swan, T. Rehren, L. Dussubieux, A. A. Eger, *Archaeometry* **2018**, *60*, 207–232.
[9] H. Ma, J. Henderson, J. Cui, K. Chen, *Adv. Archaeomaterials* **2020**, *1*, 27–35.
[10] C. Moretti, S. Hreglich, in *Mod. Methods Anal. Archaeol. Hist. Glas.*, John Wiley & Sons Ltd, Oxford, UK, **2013**, pp. 23–47.
[11] J. Henderson, M. Tregear, N. Wood, *Archaeometry* **1989**, *31*, 133–146.
[12] J. Burlot, P. Colomban, L. Bellot-Gurlet, Q. Lemasson, L. Pichon, *J. Eur. Ceram. Soc.* **2024**, *44*, 116746.
[13] M. Beltrán, F. Brock, T. Pradell, *Int. J. Appl. Glas. Sci.* **2019**, *10*, 414–425.
[14] M. Beltrán, N. Schibille, F. Brock, B. Gratuze, O. Vallcorba, T. Pradell, *J. Eur. Ceram. Soc.* **2020**, *40*, 1753–1766.
[15] M. Beltran, N. Schibille, B. Gratuze, O. Vallcorba, J. Bonet, T. Pradell, *J. Eur. Ceram. Soc.* **2021**, *41*, 1707–1719.
[16] C. Machado, M. Vilarigues, T. Palomar, *J. Cult. Herit.* **2021**, *49*, 239–249.
[17] T. Pradell, G. Molina, S. Murcia, R. Ibáñez, C. Liu, J. Molera, A. J. Shortland, *Int. J. Appl. Glas. Sci.* **2016**, *7*, 41–58.

[18] C. Machado, M. Oujja, L. Cerqueira Alves, M. Martínez-Weinbaum, L. Maestro-Guijarro, P. M. Carmona-Quiroga, M. Castillejo, M. Vilarigues, T. Palomar, *Herit. Sci.* **2023**, *11*, 85.
[19] J. Kunicki-Goldfinger, in *Annu. Rep. 2018* (Eds.: J. Michalik, E. Godlewska-Para), Institute Of Nuclear Chemistry And Technology, Warszawa, Poland, **2019**, pp. 79–80.
[20] G. Van der Snickt, O. Schalm, J. Caen, K. Janssens, M. Schreiner, *Stud. Conserv.* **2006**, *51*, 212–222.
[21] V. Devulder, P. Degryse, F. Vanhaecke, *Anal. Chem.* **2013**, *85*, 12077–12084.
[22] T. Palomar, M. García-Heras, M. A. Villegas, *Bol. Soc. Esp. Ceram. V.* **2009**, *48*, 187–194.
[23] J. Curran, T. Hicks, T. Trejos, in *Handb. Trace Evid. Anal.* (Eds.: V. J. Desiderio, C. E. Taylor, N. N. Daéid), John Wiley & Sons, Hoboken, NJ, USA, **2021**, pp. 377–420.
[24] P. Colomban, A. T. Ngo, N. Fournery, *Herit. 2022, Vol. 5, Pages 233–259* **2022**, *5*, 233–259.
[25] P. Richet, *Encycl. Glas. Sci. Technol. Hist. Cult.* **2021**, 1413–1440.
[26] N. Carmona, I. Ortega-Feliu, B. Gómez-Tubío, M. A. Villegas, *Mater. Charact.* **2010**, *61*, 257–267.
[27] H. R. Verma, in *At. Nucl. Anal. Methods*, Springer Berlin Heidelberg, Berlin, Heidelberg, **2007**, pp. 1–90.
[28] R. Acharya, S. W. Raja, S. Chhillar, J. Gupta, J. K. Sonber, T. S. R. C. Murthy, K. S. Bhushan, R. M. Rao, S. Majumdar, P. K. Pujari, *J. Anal. At. Spectrom.* **2018**, *33*, 784–791.
[29] D. A. Cremers, L. J. Radziemski, *Handb. Laser-Induced Break. Spectrosc. Second Ed.* **2013**, 10.1002/9781118567371.
[30] R. Noll, *Laser-Induced Break. Spectrosc. Fundam. Appl.* **2012**, 1–543.
[31] A. Giakoumaki, K. Melessanaki, D. Anglos, *Anal. Bioanal. Chem.* **2007**, *387*, 749–760.
[32] N. Carmona, M. A. Villegas, M. García-Heras, M. Oujja, S. Gaspard, M. Castillejo, *Proc. Int. Conf. Heritage, Weather. Conserv. HWC 2006* **2006**.
[33] N. Carmona, M. Oujja, E. Rebollar, H. Römich, M. Castillejo, *Spectrochim. Acta Part B* **2005**, *60*, 1155–1162.
[34] M. Oujja, M. Sanz, F. Agua, J. F. Conde, M. García-Heras, A. Dávila, P. Oñate, J. Sanguino, J. R. Vázquez De Aldana, P. Moreno, M. A. Villegas, M. Castillejo, *J. Anal. At. Spectrom.* **2015**, *30*, 1590–1599.
[35] M. Oujja, F. Agua, M. Sanz, D. Morales-Martin, M. García-Heras, M. A. Villegas, M. Castillejo, *Talanta* **2021**, *230*, 122314.
[36] T. Palomar, M. Oujja, M. García-Heras, M. A. Villegas, M. Castillejo, *Spectrochim. Acta Part B* **2013**, *87*, 114–120.
[37] T. Palomar, M. Martínez-Weinbaum, M. Aparicio, L. Maestro-Guijarro, M. Castillejo, M. Oujja, *Appl. Sci.* **2022**, *12*, 5760.
[38] N. Carmona, M. Oujja, S. Gaspard, M. García-Heras, M. A. Villegas, M. Castillejo, *Spectrochim. Acta Part B* **2007**, *62*, 10.1016/j.sab.2007.01.003.
[39] M. Oujja, T. Palomar, M. Martínez-Weinbaum, S. Martínez-Ramírez, M. Castillejo, *Eur. Phys. J. Plus 2021 1368* **2021**, *136*, 1–22.
[40] R. S. Harmon, J. Remus, N. J. McMillan, C. McManus, L. Collins, J. L. Gottfried, F. C. DeLucia, A. W. Miziolek, *Appl. Geochem.* **2009**, *24*, 1125–1141.
[41] T. Hussain, M. A. Gondal, *Environ. Monit. Assess.* **2008**, *136*, 391–399.
[42] E. M. Rodriguez-Celis, I. B. Gornushkin, U. M. Heitmann, J. R. Almirall, B. W. Smith, J. D. Winefordner, N. Omenetto, *Anal. Bioanal. Chem.* **2008**, *391*, 1961–1968.
[43] T. Kim, Z. G. Specht, P. S. Vary, C. T. Lin, *J. Phys. Chem. B* **2004**, *108*, 5477–5482.
[44] M. M. Suliyanti, S. Sardy, A. Kusnowo, M. Pardede, R. Hedwig, K. H. Kurniawan, T. J. Lie, D. P. Kurniawan, K. Kagawa, *J. Appl. Phys.* **2005**, *98*, 93307.
[45] I. Osticioli, M. Wolf, D. Anglos, *Appl. Spectrosc.* **2008**, *62*, 1242–1249.
[46] B. Gratuze, M. Blet-Lemarquand, J.-N. Barrandon, *J. Radioanal. Nucl. Chem.* **2001**, *247*, 645–656.
[47] D. W. Johnson, F. A. Hummel, *J. Am. Ceram. Soc.* **1968**, *51*, 196–201.
[48] A. Kramida, Y. Ralchenko, J. Reader, NIST ASD Team, *NIST Atomic Spectra Database [Online] http://physics.nist.gov/asd* **2014**, Available: http://physics.nist.gov/asd.
[49] A. Abdelouas, J. Neeway, B. Grambow, in *Springer Handb. Glas.* (Eds.: J. D. Musgraves, J. Hu, L. Calvez), Springer Cham, International Publishing, **2019**, pp. 407–438.
[50] K. Müller, H. Stege, *Archaeometry* **2003**, *45*, 421–433.

Manuscript received: October 14, 2024
Version of record online: February 3, 2025